AIP | Review of Scientific Instruments

High throughput screening by multichannel glass fiber fluorimetry

Andreas Schober, Rolf Günther, Uwe Tangen, Gaby Goldmann, Tobias Ederhof, Andre Koltermann, Anja Wienecke, Andreas Schwienhorst, and Manfred Eigen

Citation: Review of Scientific Instruments **68**, 2187 (1997); doi: 10.1063/1.1148110
View online: http://dx.doi.org/10.1063/1.1148110
View Table of Contents: http://scitation.aip.org/content/aip/journal/rsi/68/5?ver=pdfcov
Published by the AIP Publishing

Articles you may be interested in

A high-throughput cellulase screening system based on droplet microfluidics
Biomicrofluidics **8**, 041102 (2014); 10.1063/1.4886771

Optofluidic manipulation of Escherichia coli in a microfluidic channel using an abruptly tapered optical fiber
Appl. Phys. Lett. **103**, 033703 (2013); 10.1063/1.4813905

Simple fiber-optic confocal microscopy with nanoscale depth resolution beyond the diffraction barrier
Rev. Sci. Instrum. **78**, 093703 (2007); 10.1063/1.2777173

A high pressure fiber-optic reactor with charge-coupled device array ultraviolet-visible spectrometer for monitoring chemical processes in supercritical fluids
Rev. Sci. Instrum. **70**, 4661 (1999); 10.1063/1.1150129

High-efficiency and high-resolution fiber-optic probes for near field imaging and spectroscopy
Appl. Phys. Lett. **71**, 2886 (1997); 10.1063/1.120206

This article is copyrighted as indicated in the article. Reuse of AIP content is subject to the terms at: http://scitationnew.aip.org/termsconditions. Downloaded to IP: 134.76.223.157 On: Tue, 06 Oct 2015 10:04:36

High throughput screening by multichannel glass fiber fluorimetry

Andreas Schober[a)]
Institut für Molekulare Biotechnologie, Beutenbergstrasse 11 07745 Jena, Germany

Rolf Günther
Evotec, Grandweg 64, 22529 Hamburg, Germany

Uwe Tangen
Institut für Molekulare Biotechnologie, Beutenbergstrasse 11 07745 Jena, Germany

Gaby Goldmann, Tobias Ederhof, and Andre Koltermann
Max-Planck-Institut für Biophysikalische Chemie, Postfach 2841, 37018 Göttingen, Germany

Anja Wienecke
Evotec, Grandweg 64, 22529 Hamburg, Germany

Andreas Schwienhorst
Institut für Molekulare Biotechnologie, Beutenbergstrasse 11 07745 Jena, Germany

Manfred Eigen
Max-Planck-Institut für Biophysikalische Chemie, Postfach 2841, 37018 Göttingen, Germany

(Received 19 October 1995; accepted for publication 12 February 1997)

As a tool for screening large numbers of biological samples by means of amplification (e.g., $Q\beta$ or PCR) we have constructed a thermocycler that includes optionally a 96-channel or 960-channel glass fiber fluorimeter (combined with a cooled charge-coupled-device camera). We briefly describe the system integration of all components like liquid handling, thermostats, an x,y,z robot arm, and the glass fiber fluorimeter. The integrated glass fiber fluorimeter allows sensitive on-line measurements in 960 channels within 5 s. Two different screening procedures were carried out. In a first experiment PCR reactions were done in the presence of the known PCR inhibitor hematin and its suppressor transferrin. The system was used to titrate the suppressor with the inhibitor hematin in order to determine the maximum inhibitor concentration tolerated at a given suppressor concentration. We processed 96 PCR samples in parallel with 11 different concentration steps. In a second experiment the 960-channel glass fiber fluorimeter was used to monitor on line the amplification of the $Q\beta$ system in the presence or absence of an inhibitor (heparin). Since the doubling time of $Q\beta$ RNA variants is about 20 s, on-line detection is crucial for the experimental setup. The evolution of new RNA species adapted to high inhibitor concentrations could be proved by comparison of the fluorimetric signal and electrophoresis. © *1997 American Institute of Physics.* [S0034-6748(97)04305-0]

I. INTRODUCTION

In recent years high-throughput screening has become a driving force in drug development and diagnostics. Clearly there is now a demand for automated systems that can assess huge numbers of samples in a minimum amount of time by means of relevant assays.[1–5]

Within the scope of different screening assays biological amplification systems have now become significantly important. *In vivo* assays based on amplification of cells like classical antibiotic screenings or screening with genetic engineered cells, i.e., transactivation assays[6,7] as well as *in vitro* assays based on amplification of nucleic acids like $Q\beta$[8,9] PCR exhibit wide range of applications.

PCR, for example, is used in a broad range of applications, such as gene detection for analytical purposes as well as rapid preparation of large amounts of modified DNA[10,11] in the evolutionary biotechnology.[12,13] Unfortunately, it very often appears to be necessary to screen the concentrations of enzyme, primers, nucleotides, and bivalent ions, and the cycling schedule must also be varied to find the optimal PCR protocol,[14] which can be time consuming if carried out sequentially.

Many automated systems have been developed with accurate temperature cycling and with automated process control in appropriate reaction vessels[4,15–18] for pure PCR applications, but there are only a few systems[19] that are capable of analyzing on-line the success of a PCR protocol. On-line analysis should reduce significantly the work required for screening and would decrease the costs correspondingly.

Furthermore such machines are very often constructed on a certain purpose and do not exhibit a flexibility versus other applications such as isothermal amplifications *in vivo* and *in vitro* like in the $Q\beta$ or the 3SR system.[20,21]

For a more flexible performance high-throughput screening devices should also contain instruments of determining the kinetics of amplification as well as quantifying target concentrations on line and accurately. This can be achieved by using fluorimetric methods, i.e., serial scanning systems[22,23] or charge-coupled devices (CCDs) working in parallel.[19] For a review see Warner *et al.*[24]

Cooled CCD cameras have been developed for astronomy and are important tools in spectroscopy.[25] They

[a)]Author to whom correspondence should be addressed.

This article is copyrighted as indicated in the article. Reuse of AIP content is subject to the terms at: http://scitationnew.aip.org/termsconditions. Downloaded to IP: 134.76.223.157 On: Tue, 06 Oct 2015 10:04:36

were introduced in biology since the late 1980s[26,27] and used in flow cytometry,[28,29] in light microscopy,[30,31] and in confocal scanning microscopy.[32,33] CCDs are also widely applied in the field of electron microscopy (see, for example, Refs. 34 and 35).

Measurements in neurobiology[36] and hybridization experiments[37,38] were performed with CCDs. Bioluminescence measurements were also practiced.[39,40] An overview is given by Earle *et al.*[41] and by Warner and co-workers.[24]

The machine described in this report combines automatic sample preparation, automatic temperature and process control, and, as the most important part, on-line detection. The design of the machine was constrained by the widespread microtiter norm as a standard in laboratory automation (i.e., pipetting robots and reaction vessels). Illumination and detection of samples spread on a large area defined by the space needed for ten microtiter plates caused a problem of its own. As a suitable solution we constructed a multichannel glass fiber fluorimeter combined with a CCD camera. Similar approaches, also in other applications—although on much smaller degree of parallelism—have been published previously.[42,43] Similar approaches are known in the field of fiber optic sensors.[44]

The machine is able to guarantee each arbitrary processing temperature up to 120 °C. Furthermore it cycles the temperature automatically for PCR applications and has the capacity to carry up to 960 samples in an integrated array of sealed, disposable plastic reaction vessels; the liquids are handled automatically with an integrated pipetting robot[17] and can be measured by an integrated 960-channel (optionally a 96-channel) glass fiber fluorimeter. Optical measurements are within 5 s in all 960 channels.

We demonstrate the function of the machine with a 96-channel PCR experiment detecting the inhibitor (hematin) dependence of our PCR system. The performance of the 960-channel fluorimeter was shown with the on-line measurement of the $Q\beta$ *in vitro* amplification. As an example of the influence of an inhibitor (heparin) on the kinetics of $Q\beta$, we practiced a 96-channel experiment with three different heparin concentrations.

II. INSTRUMENTATION AND MATERIALS

The system has to perform following processes (see Fig. 1): sample preparation, sample processing, on-line analysis (screening). The main components due to the described tasks are listed in the following

Tools for sample preparation include: plastic reaction vessels: a plastic sheet with 96 reaction vessels (see Sec. II C 1); a heat sealer to seal the PCR samples in the reaction vessels; a liquid delivery system with two independent pipetting robot arms: one arm with an 8-channel adapter with eight disposable tips and one 1-channel arm with an adapter for disposable cannulas (Fig. 2); a transportation unit for moving the sample carrier between the different pipetting and temperature stations that can hold up to 10 plastic sheets (i.e., a total of 960 samples) (Fig. 2).

Components of the temperature control, include three thermostats to perform the temperature adjustments required for the polymerase chain reaction and a freeze-storage device to store the reaction solutions for further analysis (Fig. 2).

Tools for the process control and the fluorimeter include: a process control unit with several computers based on the Versa Module Eurocard (VME) data bus; a glass fiber fluorimeter with 960 excitation and 960 emission fibers (optionally a 96-channel fluorimeter is available) [Fig. 3(b)]; a CCD camera and on-line image processing software by the VME data bus computer (Fig. 2).

The central part of this machine is the system integration of all processes directed by the VME bus computer (Fig. 4) with the master CPU chip 68020 (Motorola). The experiments are controlled in the fluorimeter via the image processing language (TCL). This language has been expanded with commands for controlling the pipetting robot, the computer numeric control (CNC) positioning device, the temperature controllers (Dicon 1, Dicon 2), a PT100 measurement card, various relais, sensors and valves (EKF VME 68200).

A. Principles of fluorimetric measurement with a glass fiber fluorimeter: Theoretical aspects

The amplification of nucleic acids can be measured by the enhanced fluorescence of the bound dye molecules in the nucleic acid strands.

The relative change of the fluorescence signal is with a given ethidium bromide (EtBr) concentration C^0_{EtBr} proportional (expressed by the constant factor V) to the concentration of bound EtBr(C^b_{EtBr}),

$$\frac{I-I_0}{I_0}=(V-1)\,\frac{C^b_{\mathrm{EtBr}}}{C^0_{\mathrm{EtBr}}}\,. \tag{1}$$

Thus, the fluorescence signal of the concentration of bound EtBr is coupled via the mass action law to the concentration of the nucleic acids,

$$K=\frac{C^b_{\mathrm{EtBr}}}{(C^0_{\mathrm{EtBr}}-C^b_{\mathrm{EtBr}})(nC_n-C^b_{\mathrm{EtBr}})}\,, \tag{2}$$

$$\frac{I-I_0}{I_0}=(V-1)\,\frac{C^0_{\mathrm{EtBr}}+nC_n+K^{-1}}{2C^0_{\mathrm{EtBr}}} +\left(\frac{C^0_{\mathrm{EtBr}}+nC_n+K^{-1}}{4}-nC^0_{\mathrm{EtBr}}C_n\right)^{1/2}, \tag{3}$$

where n is the number of the EtBr binding sites and K the equilibrium constant of the binding sites of EtBr.

With the following simplifications:

$$C_b^2=\ll nC^0_{\mathrm{EtBr}}C_n\,,\quad C^0_{\mathrm{EtBr}}\approx(C^0_{\mathrm{EtBr}}+nC_n), \tag{4}$$

one yields with Eq. (2) the following (linear) approximation between EtBr and the RNA concentration $C_n(t)$:

$$\frac{I-I_0}{I_0}=\frac{n(V-1)}{C^0_{\mathrm{EtBr}}+K^{-1}}\,C_n(t). \tag{5}$$

If one computes $\ln[(I-I_0)/I_0]$, one can yield very easy the rate constants for the individual channels from the slope of the line.[45]

This article is copyrighted as indicated in the article. Reuse of AIP content is subject to the terms at: http://scitationnew.aip.org/termsconditions. Downloaded to IP: 134.76.223.157 On: Tue, 06 Oct 2015 10:04:36

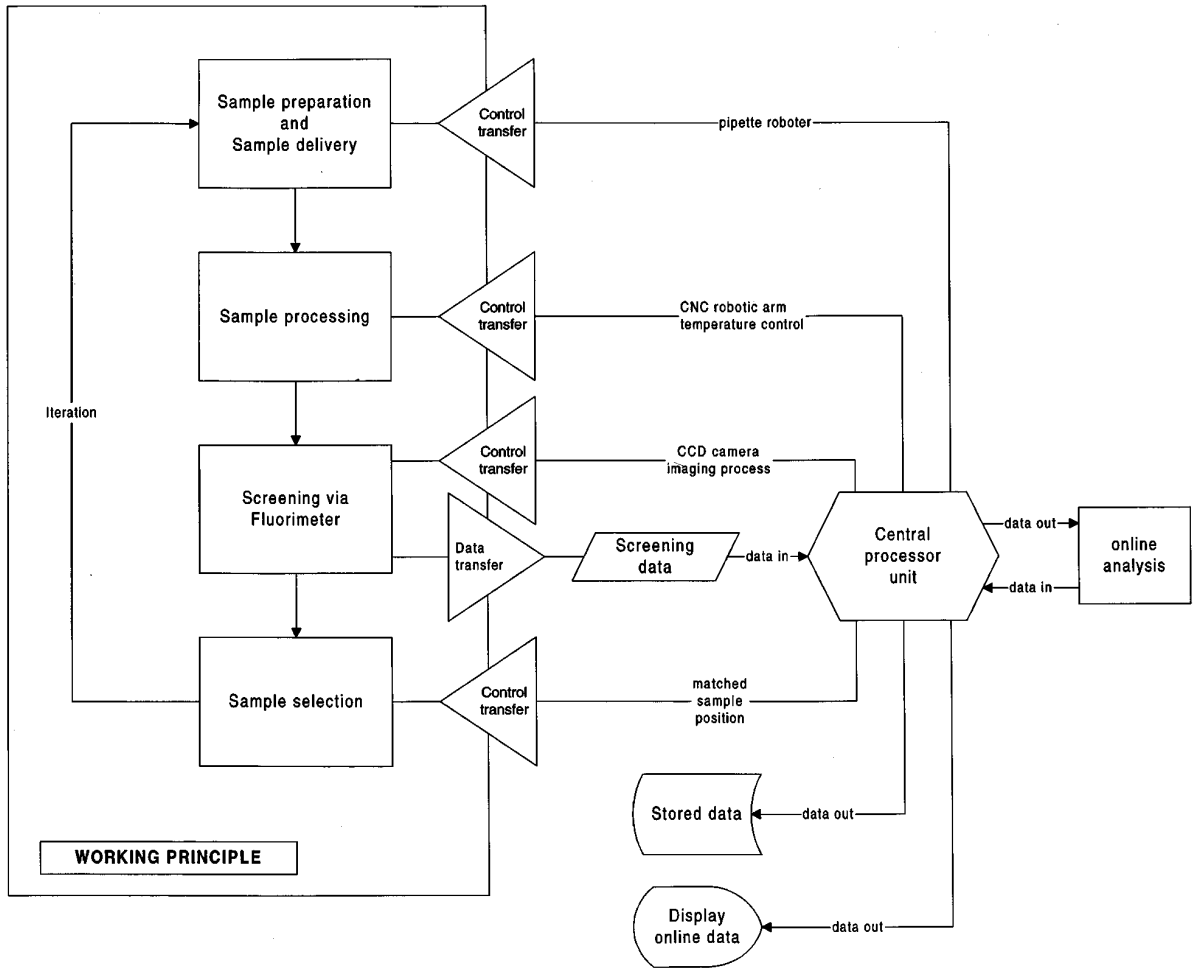

FIG. 1. Sketch of the whole screening process (left-hand side). The arrows indicate the different processing and control units, which are used for the automatic screening process (right-hand side).

B. Optics: Why a glass fiber fluorimeter?

Fluorescence emission can be detected in many different ways. The design of our instrument is constrained by the following features: The simultaneous measurement of 960 separate channels (optionally 96) is achieved best with a planar array of the samples; because of its frequent use, we wish to use the microtiter norm with set volumes, and this together with the necessity of different positions with different temperatures sets a limit on the minimum size of the instrument; the planar design renders the normal orthogonal arrangement of the excitation and emission light pathways impractical; the mobility of the lid of the thermal block where the detection takes place made flexible optical pathways necessary.

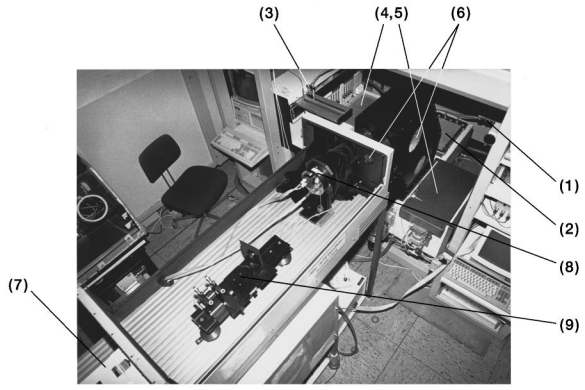

FIG. 2. Photo of the machine. The transportation unit (1) moves the sample carrier (2) between the different pipetting (3) and temperature stations (4),(5). The position in the middle shows the fluorimeter with the 960 glass fibers inside (6). In front one can see the laserhead (7), the CCD system (8), and the aspheric mirrors with the microscopic objective (9).

The packing density of the separate samples is set by the microtiter norm of 75.97 cm^2 for 96 chambers. Each chamber has an area of about 0.28 cm^2. The area used by the samples is only 27.14 cm^2; 48.83 cm^2 are lost to the space between the wells. If the total area of the microtiter sheets is illuminated, the intensity of the excitation light for exciting a reasonable fluorescence intensity must be 2 to 3 times the intensity that is necessary for illuminating only the area actually taken up by the samples.

If the 96 fibers are packed in an area of 6.2 cm^2, (which is a diameter of 2.8 cm), the energy density is 0.16 W/cm^2, which is 18 times the energy density that would be achieved by illuminating the area of 114.4 cm^2 of a single plastic sheet. If we illuminate the total area of $44 \times 26\ cm^2 = 1144\ cm^2$ (10 plastic sheets with the microtiter measure) with a laser power of 1 W the illumination density

This article is copyrighted as indicated in the article. Reuse of AIP content is subject to the terms at: http://scitationnew.aip.org/termsconditions. Downloaded to IP: 134.76.223.157 On: Tue, 06 Oct 2015 10:04:36

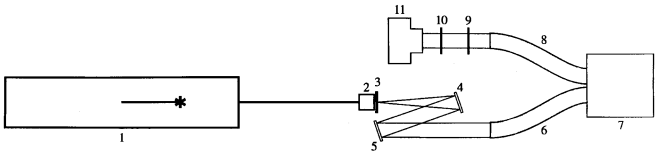

(a)

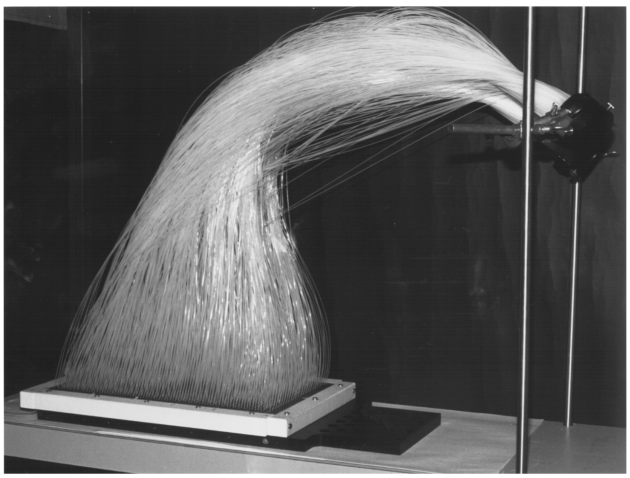

(b)

FIG. 3. (a) Scheme of the optical device. The beam of the Ar^+ ion laser (1) is focused by a microscope objective (2) onto a pinhole (3). The expanded laser beam distribution is transformed by the aspheric mirrors (4),(5). The light is then coupled into the fiber bundle (6) and then distributed onto the sample carrier with its matrix of samples. The fluorescence light (600 nm) is detected by another bundle (8) and the emerging light passes through a combination of an interference (9) and an absorption filter (10). A Zeiss camera lens focuses the image onto the CCD (11). (b) Photo of the 960-channel glass fiber fluorimeter. One can see the two bundles: the emission and the excitation branch.

is only 8.74×10^{-4} W/cm^2. If a bundel of 960 fibers is packed in an area of 23 cm^2 (a circle with a diameter of 5.4 cm), and the laser beam is expanded to this area, this corresponds to a light density of 0.04 W/cm^2; This light density is 46 times greater than the energy density calculated above.

A similar argument pertains to the detection of the fluorescence emission. By employing optical glass fibers many separate reaction chambers can be measured independently of each other.

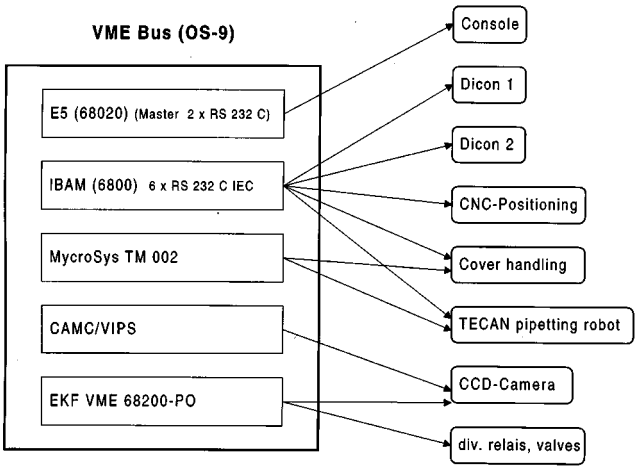

FIG. 4. This block diagram is only the sketch of the fluorimeter. The arrows indicate communication links. Most of them are standard RS-232-C serial connections.

1. The CCD detector

The detection device and the computer-based image processing must fulfill the following conditions: on-line process control and image processing; parallel data aquisition and analysis; high sensitivity; high compatibility with the fiber bundle.

The system that has been selected (H. R. Tietz GmbH, Gauting bei München) consists of a VME bus computer, an image processing software TCL (University of Eindhooven), and a Photometrics CCD camera (Tucson, Arizona).

The CCD camera contains a Thomson THX 31156 CCD chip with 1024×1024 square pixels each with an area of 19×19 μm^2; the sensitivity is 3.3 μV cm^2/J corresponding to 1.5 μV/e$^-$ (Thomson-CSF, 1987).

The 14 bit analog-to-digital conversion of the CCD signals takes place at 50 kHz, and by ''binning'' (adding neighboring pixels into superpixels, e.g., adding 4×4 pixels into a single superpixel with the sum of 16 pixels), the pixel number can be reduced to 65 536 pixels; this results theoretically in a total readout time of about 1.3 s. For 1000 channels a fourfold binning should suffice.

2. Excitation branch

The argon ion laser (Lexel Lasers) is operated in the TEM_{00} mode, which has a radially symmetric Gaussian intensity distribution. The laser beam, which has an original diameter of 1.3 mm, is expanded by a microscope objective; the output of the objective is focused onto a pinhole to filter out the unwanted modes. The divergent laser beam emerging from the pinhole is then transformed from a Gaussian profile into a rectangular profile by a specially developed optical system consisting of aspheric mirrors; the surfaces of these mirrors have been calculated numerically to produce a rectangular profile [see Figs. 2 and 3(a)]. This ensures a homogeneous distribution of light intensity across the surface. The mirrors were constructed by Zeiss, Oberkochen using the computed parameters.

3. Construction of the fiber bundles

As a first step we constructed a 96-channel fiber bundle; each channel consists of one excitation and one emission fiber, each 1 m long. The fibers are cut from a single reel of fiber. The Teflon coating at the end of each fiber is removed and then smoothed and polished. The fibers are fixed on their one end with a two component glue in two masks (one mask for excitation and one for emission) and then fixed in the head of the measurement unit (consisting of the sample carrier and the cover plate with excitation and emission bundles). In addition, the fibers are monocled in a heatproof matrix of ceramic glue on top of the measurement unit [Fig. 3(b)].

The geometry of the measurement chamber is designed so that the axis of the emission fiber is normal to the surface of the sample chamber, and symmetrically orientated in the

This article is copyrighted as indicated in the article. Reuse of AIP content is subject to the terms at: http://scitationnew.aip.org/termsconditions. Downloaded to IP: 134.76.223.157 On: Tue, 06 Oct 2015 10:04:36

center of the head, whereas the axis of the excitation fiber is oriented at an angle of 15° from the emission fiber. Multiple reflections of the excitation light should lead to a nearly homogeneous illumination of the solution. One can expect the maximum intensity of the emission light to be emitted normal to the surface. The usual arrangement for a fluorimeter with the emission detection perpendicular to the excitation source could not be realized because of the parallel detection of many channels. The 15° angle was determined experimentally to be optimal.

4. Emission branch of the fluorimeter

The fluorescence emission passes through several optical components before reaching the CCD detector. After emerging from the emission fiber bundle, the fluorescence light passes through a combination of antireflection-coated interference filters and an absorption filter with an overall transmission greater than 90% at 610 nm (this is optimal for the emission of EtBr bound to DNA). A Zeiss camera lens focuses the image onto the CCD.

5. Image processing

The following image processing problems must be solved.

Every illuminated pixel must be assigned to the single fiber. Such an assignment (''mask'') must be carried out automatically.

Computation, normalization, and simultaneous readout is necessary to compare the channels.

Every channel must be allocated to a group of pixels in the pixel matrix (image segmentation problem). Without any background information the expected image can be extracted from the noisy image with the help of threshold algorithms: If the intensity of a pixel is greater than the threshold, then the pixel is identified as a channel pixel; otherwise it is set to 0. Such thresholds can be fixed or determined by several statistical methods. Tools are supplied by the TCL–Tietz software system. Such methods can be found in Refs. 46 and 47.

C. Sample preparation and handling of liquids

1. Sealing the samples

The sealed plastic reaction vessels ensure fast processing of each sample under identical conditions and avoid evaporation and cross contamination. The reaction chambers are made from films extruded from Macrolon (Kunststoffe Arthur Krüger, Hamburg, FRG); these are chemically inert and have negligible fluorescence. The finished and sealed reaction vessels have a volume of 40 μl; the thickness of the wall is 40 μm. The plastic reaction vessels must be sealed after the wells have been filled with the biochemical reaction solution. A heat sealer welds a 100-μm-thick Macrolon coverfoil to the sheet containing the plastic reaction vessels. Details concerning the process of forming the foils, the welding machine, and the effect of the heat sealing process on the biological material can be found in Ref. 17.

2. Delivery system for the liquids

A pipetting robot RSP 5052 (Zinsser Analytic, Tecan Robotics, Frankfurt, FRG) delivers the samples to the plastic sheets before they are sealed.

The computer controlled pipetting process allows the pipetting of up to four separate solutions to the plastic sheet with the reaction chambers with the eight-channel arm of the robot. By adjusting the relative volumes of two solutions a concentration gradient of, for instance, an inhibitory substance can be achieved in the final reaction mixture.

3. Transportation unit and sample carrier

For convenient sample handling we use an x,y,z manipulator (CNC machine 82 V4: Föhrenbach, Löffingen, FRG); this transports the sample carrier ($444\times260\times5\ \mathrm{mm}^3$) between the three different temperature stations required for the PCR reaction. One temperature station is equipped with an optical detection device (see Sec. II B). The sample carrier contains up to 10 plastic sheets with 96 reaction vessels each.

4. Thermostating and freeze storage facilities

All thermostats are constructed from large aluminum blocks ($490\times270\times290\ \mathrm{mm}^3$) that provide a high heat capacity and guarantee temporal and spatial temperature homogeneity.[17] The desired temperatures are maintained either by heating elements placed inside the blocks or by circulating cooling water. The temperature of the sample carrier is measured by a Pt 100 thermocouple probe fixed to the sample carrier with silicon glue. After moving the samples to the appropriate thermostats, the sample carrier is pressed onto the chosen aluminum block by a vacuum system integrated into each block. Tempered cover plates ensures all over temperature control.

Details of the thermodynamic properties are given in Ref. 17.

D. Biochemistry: PCR and $Q\beta$ amplification as test procedure

The sequence of the Tetrahymena group I intron was used as a target sequence for this study. Primer sequences are listed in Ref. 14. The standard PCR reaction mix contained buffer (GeneAmp kit, Perkin Elmer Cetus Corporation, Norwalk, CT), 1.5 mM $MgCl_2$, 10 μM of each primer, 200 μM dNTPs, 100 ng of template pT71-21Sca and 6 units of Taq polymerase (Amersham Buchler, Braunschweig).

Hematin and transferrin (both by Boehringer Mannheim) were added as indicated.[14] Usually 30 cycles were accomplished using the following protocol: denaturation at 94 °C for 1.5 min, annealing at 55 °C for 2 min, and extension at 72 °C for 2.2 min. The same mixture was cycled in a commercially available thermocycler; the solution was overlaid with 50 μl mineral oil before starting the PCR. The products were analyzed on 0.8% agarose gels. DNA was made visible by ethidium bromide staining and exposure to UV light.

The wells of the plastic reaction vessels were filled to a final volume of 30 μl each by combining different volumes of hematin PCR mixture and PCR transferrin mixture. From

This article is copyrighted as indicated in the article. Reuse of AIP content is subject to the terms at: http://scitationnew.aip.org/termsconditions. Downloaded to IP: 134.76.223.157 On: Tue, 06 Oct 2015 10:04:36

row 2 to row 12 the amount of hematin PCR mixture is increased in steps of 3 μl. The pipetting robot can discharge both solutions at every rack position. Because the same amount of transferrin (0.156 mg/ml) is pipetted at every position the transferrin concentration is constant whereas the hematin concentration is increased by 3.2 μM at every consecutive step; the concentration increases from 0 μM in the second row to 32 μM in the 12th row. Wells 1–8 were pipetted by hand in order to show that the automatic pipetting facility does not affect the results. Wells 1–4 contain no hematin and 0.156 mg/ml transferrin; in wells 5–8 no hematin and no transferrin were used.

After the pipetting has been carried out the plastic sheets are sealed by the sealing machine with a sealing time of 10 s at 273 °C. Previous measurements have shown that only the temperature outside of the wells was raised; the solution inside the wells was not affected. The solution temperature does not exceed 90 °C during sealing operation.

The PCR solutions contain 3 μM EtBr and were analyzed on line by the glass fiber fluorimeter and on 0.8% agarose gels as described above. The agarose gels were analyzed with a densitometer (Millipore Waters) and compared with the fluorimeter results.

On-line fluorescence detection (not done in the Biometra thermocycler) confirmed the results of gel electrophoresis. The addition of 0.156 mg/ml transferrin leads to positive results in both machines and with both detection methods (Biometra: again only gel electrophoresis was used) despite hematin concentrations up to 8 μM.

As an example of time sensitive evolutionary amplification systems RNA variants of the *in vitro* $Q\beta$ system were amplified parallally in 960 channels to test the fluorimeter. Furthermore the influence of the inhibitor Heparin was analyzed amplifying $Q\beta$ in the presence of different concentration of the inhibitor heparin.[47] The RNA sequences and biochemical details are listed in Ref. 17. The RNAs were amplified in presence of 0, 20, and 40 μM heparin in three groups of 32 samples each during the heparin experiment. The different sample handling of the RNAs is described in Ref. 17.

III. RESULTS

Standard PCR amplification was completely abolished at hematin concentrations as low as 0.7 μM provided that no transferrin is present. This was also observed for the commercially available Biometra thermocycler as well as the multichannel fluorescence machine.

The presence of 0.156 mg/ml transferrin drastically suppressed inhibition in both machines.

Titration experiments in the Biometra thermocycler determined reproducibly the threshold for positive amplification with no more than 22.6 μM hematin at the given transferrin concentration.

In Fig. 5 the normalized fluorescence intensities (arbitrary units) are mapped onto the channel number and to the time axis. One can observe the dynamics of the time course of the PCR process. From channels 9 to 96 the hematin concentration of the solution increases in 11 steps as described

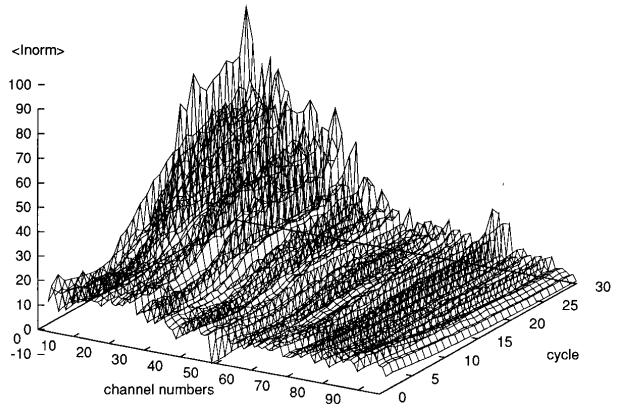

FIG. 5. Time resolved multichannel PCR amplification study. Normalized fluorimetric signals (arbitrary units) are mapped to the channel number and the time axis. The hematin gradient is increasing from channel 13 to channel 96. In channels 1–12 no hematin is pipetted.

in Sec. II. Therefore the efficiency of the PCR amplification is decreased.

Despite the large variance one can observe the effect of the concentration of hematin on the dynamics of the amplification. The 96 channels are divided into groups of 8 consecutive channels, and all channels in each group contain the same solution. The mean values of the intensities of the channels in the last PCR cycle with the same concentrations (e.g., the 11 rows) are plotted versus the increasing hematin concentrations (see Fig. 6).

The results of evaluating the gel photographs with a densitometer as described in Sec. II are given in Fig. 7, which has approximately the same shape as Fig. 6. The variance of the densitometer analysis is smaller by a factor of 3 than the variance of the glass fiber fluorimeter analysis. This might be the result from the high EtBr concentration during EtBr gel staining and long illumination times. The optical difference between the welded plastic reaction vessels is another possible contributing factor. The differences between the single fibers which have been individually polished is minimized by the normalization of the single intensities.

Nevertheless, the success of the PCR amplification as a

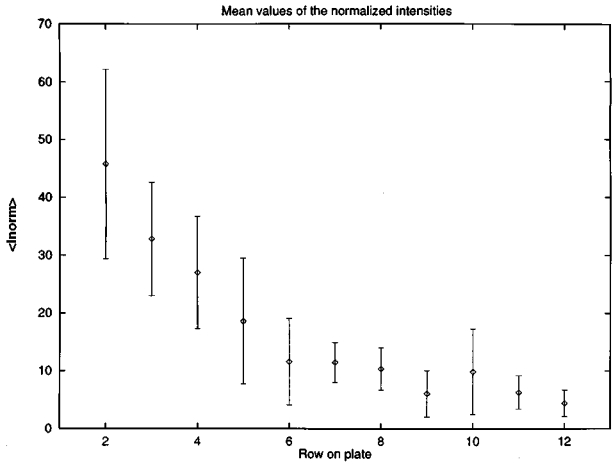

FIG. 6. Measurement of the glass fiber fluorimeter. Mean values of the channels with the same concentrations are plotted vs the increasing hematin concentrations.

This article is copyrighted as indicated in the article. Reuse of AIP content is subject to the terms at: http://scitationnew.aip.org/termsconditions. Downloaded to IP: 134.76.223.157 On: Tue, 06 Oct 2015 10:04:36

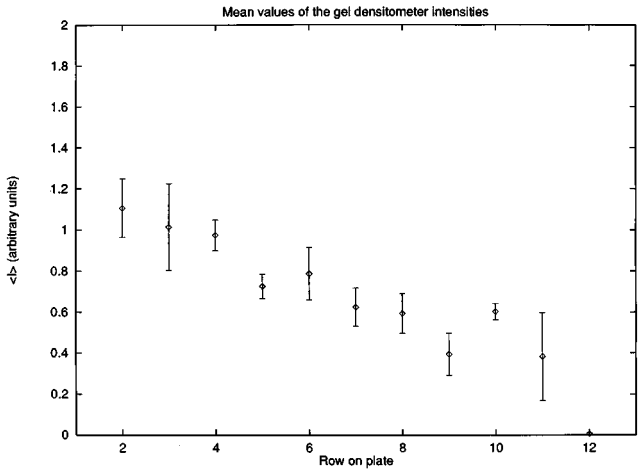

FIG. 7. Measurement of the gel densitometer. Mean values of the channels with the same concentrations are plotted vs the increasing hematin concentrations: densities of the lanes.

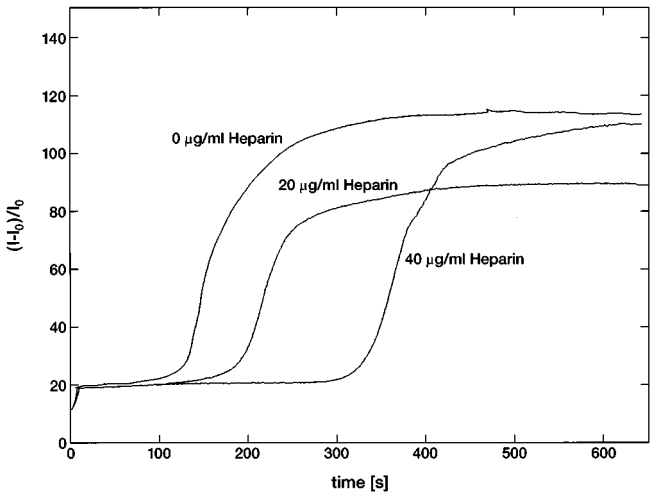

FIG. 9. Comparison of the $Q\beta$ amplification for three different heparin concentrations.

function of inhibitor concentrations can be determined by a fluorimeter before analyzing the products on a gel, which is much more time consuming.

The RNA $Q\beta$ replicase system was monitored by fluorescense measurements with the glass fiber fluorimeter (Fig. 8). One can see the homogeneous growth of the $Q\beta$ clones in all 960 channels, which can be proved by gel electrophoresis (data not shown). The computation and the analysis of the kinetics of $Q\beta$ is demonstrated with the heparin example. The effect of the increasing values of heparin is shown in Fig. 9. Heparin causes significantly a time delay in the starting point of the $Q\beta$ growth. The time delay is dependent on the heparin concentration. The amplification of the $Q\beta$ strands in the single channels affects the kinetics as one can see at the shape of the growth functions. The optical device is able to take each 4 s an image of all 960 channels with an illumination time of 150 ms. All channels can be compared by image processing within 2 s.

Gel electrophoresis reveals the evolution of new short stranded self-amplifying RNA species also reflected by an elongated initial lag phase in the growth curve (data not shown).

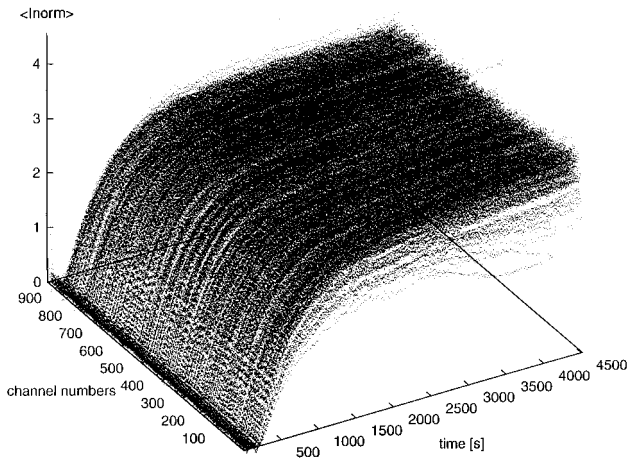

FIG. 8. Measurement of the $Q\beta$ amplification in all 960 channels. Normalized intensities (the error between signals from the 960 channels for the last image was 12.2%).

The rate constants of three selected channels are determined with equation (5) to $\kappa_0 = 0.0296\ s^{-1}$ (0 μg/ml heparin), $\kappa_{20} = 0.0224\ s^{-1}$ (20 μg/ml heparin), and $\kappa_{40} = 0.0217\ s^{-1}$ (40 μg/ml heparin). The time lag of the growth of the RNAs for the different heparin concentrations is for 0 μg/ml heparin 115.98 s for 20 μg/ml heparin 175.24 s, and for 40 μg/ml heparin 320.13 s.

IV. DISCUSSION

The PCR inhibitory studies (hematin, biliverdin, bilirubin, transferrin[14]) require screening devices that reduce the effort expanded in titration experiments. In the present study we have succeeded in screening the PCR hematin–transferrin system with an automated PCR machine consisting of an integrated glass fiber fluorimeter. This device with this optical setup is especially suited for continuous monitoring the whole amplification process of self-replicating molecules as shown in the case of the $Q\beta$ experiments.

The glass fiber fluorimeter is a robust tool in combination with our plastic microtiter foils. The time scale of one measurement is within 6 s, whereas the doubling time of $Q\beta$ is about 20 s. New CCD cameras with modern VME bus computers (Motorola master chip: 68060) can even store a 256×256 image within 0.5 s. The time scale of one measurement is within 1 s. Serial microscopic scanning systems are more sensitive, but would need a processing time destinct below 100 ms including movement and measurement to reach similar values.

The improvement and optimization of on-line, parallel sample screening should reduce the cost for testing many samples. Only those variants that will give reasonable fluorescence signals will be further analyzed. On-line measurements should provide selection criteria for screening and will be a tool for serial dilution experiments in evolutionary biotechnology. Evolutionary biotechnology is based on the principle of selection whereby replicating molecules, viruses, micro-organisms, or cell populations are subjected to externally controlled selection pressures.[12,13] In this way biologi-

This article is copyrighted as indicated in the article. Reuse of AIP content is subject to the terms at: http://scitationnew.aip.org/termsconditions. Downloaded to IP: 134.76.223.157 On: Tue, 06 Oct 2015 10:04:36

cal macromolecules can be optimized for a specific application.[48–56] To optimize selected traits of these molecules large numbers of molecules in isolated compartments must be screened.[13] Different species must be studied under identical reaction conditions and, vice versa, the evolution of one species must be observed in different environments. Data obtained from these analyses can suggest new strategies for optimization,[57] which can be provided by a fully automated system consisting of sample preparation and on-line monitoring, as shown above, and selection.[17]

Further research concerns the application of our experimental setup to *in vivo* cell based amplification systems.

Miniaturization down to the sub-μl range should reduce the costs for screening significantly.[58] Nevertheless such miniaturized screening methods have to be brought up to a macroscopic level for further analysis. Furthermore combining this techniques with the microtiter norm should allow one to practice all introduced laboratory automation and analysis.

ACKNOWLEDGMENTS

The authors are very grateful to Wolfgang Simm and his technical group as well as Roderich Weise for their help in constructing the instrument. Helpful discussions with Peter Sparllinek (Tietz image processing) concerning image processing are gratefully acknowledged. The authors thank Margitta Clegg for carefully reading the manuscript. This work was supported financially by the Bundesministerium für Forschung und Technologie, Germany (Grant No. 0310248A) and the Volkswagon foundation.

[1] M. A. Gallop, R. W. Barrett, W. J. Dower, St. P. A. Fodor, and E. M. Gordon, J. Med. Chem. **37**, 1233 (1994).
[2] E. M. Gordon, R. W. Barrett, W. J. Dower, St. P. A. Fodor, and M. A. Gallop, J. Med. Chem. **37**, 1385 (1994).
[3] R. N. Waterhouse, D. J. Silock, and L. N. Glover, Lett. Appl. Microbiol. **16**, 36 (1993).
[4] S. Meier-Ewert, E. Meier, A. Akmadi, J. Curtis, and H. Lehrach, Nature (London) **361**, 375 (1993).
[5] D. C. Uber, J. M. Jaklevic, E. H. Theil, A. Lishanskaya, and M. R. McNeely, Biotechniques **11**, 642 (1991).
[6] D. Metzger, J. H. White, and P. Chambon, Nature (London) **334**, 31 (1988).
[7] M.-E. Meyer, C. Qurin-Strickert, T. Lerouge, M.-T. Bocquel, and H. Gronemeyer, J. Biol. Chem. **267**, 10 882 (1992).
[8] Y. Wu, D. Y. Zhang, and F. R. Kramer, Proc. Natl. Acad. Sci. USA **89**, 11 769 (1992).
[9] D. J. Kenan, D. E. Tsai, and J. D. Keene, Trends Biochem. Sci. **19**, 57 (1994).
[10] M. A. Innis, D. H. Gelfand, J. J. Sninsky, and T. J. White, *PCR Protocols—A Guide to Methods and Applications* (Academic, San Diego, 1990).
[11] D. H. Saiki, O. Gelfand, S. Stoffels, S. J. Scharf, R. Higuchi, G. T. Horn, K. B. Mullis, and H. A. Erlich, Science **239**, 487 (1988).
[12] M. Eigen and W. C. Gardiner, Jr., Pure Appl. Chem. **56**, 967 (1984).
[13] M. Eigen, Chem. Scr. **26**, 13 (1986).
[14] A. Schwienhorst, A. Wienecke, and B. F. Lindemann (unpublished).
[15] P. C. Giordano, R. Fodde, M. Losekoot, and L. F. Bernini, Technique **1**, 16 (1989).
[16] H. R. Garner, B. Armstrong, and D. M. Lininger, Biotechniques **14**, 112 (1993).
[17] A. Schober, N. G. Walter, U. Tangen, G. Strunk, T. Ederhof, J. Dapprich, and M. Eigen, Biotechniques **18**, 652 (1995).
[18] S. Ponder, T. Pappas, W. J. Wells, E. Kam, A. McKay, B. S. Keenan, and C. S. Watson, Technique **2**, 202 (1990).
[19] R. Higuchi, C. Fockler, G. Dollinger, and R. Watson, Bio/Technology **11**, 1026 (1993).
[20] S. Spiegelman, Q. Rev. Biophys. **4**, 213 (1971).
[21] M. Gebinoga and F. Oehlenschlaeger, Eur. J. Biochem. **235**, 256 (1996).
[22] M. Eigen and R. Rigler, Proc. Natl. Acad. Sci. USA **91**, 5740 (1994).
[23] D. E. Koppel, F. Morgan, A. E. Cowan, and J. H. Carson, Biophys. J. **66**, 502 (1994).
[24] I. M. Warner, St. A. Soper, and L. B. McGown, Anal. Chem. **68**, 73R (1996).
[25] J. V. Sweedler, R. B. Bilhorn, P. M. Epperson, G. R. Sims, and M. B. Denton, Anal. Chem. **40**, 282 (1988).
[26] D. J. Arndt-Jovin, M. Robert-Nicoud, S. J. Kaufman, and T. M. Jovin, Science **230**, 247 (1985).
[27] Y. Hiraoka, D. A. Agard, and J. W. Sedat, Science **231**, 36 (1987).
[28] J. A. Steinkamp, T. M. Joshida, and J. C. Martin, Rev. Sci. Instrum. **64**, 3440 (1993).
[29] F. Kubota, H. Kusuzawa, T. Kosaka, and H. Nakamoto, Cytometry **21**, 129 (1995).
[30] St. Herr, Th. Bastian, R. Pepperkok, Ch. Boulin, and W. Ansorg, Methods Mol. Cell. Biol. **4**, 164 (1993).
[31] M. Ambroz, A. J. MacRobert, J. Morgan, G. Rumbles, M. S. C. Foley, and D. Philipps, J. Photochem. Photobiol. B **22**, 105 (1994).
[32] M. I. Highett, D. J. Rawlins, and P. J. Shaw, Cell Sci. **104**, 843 (1993).
[33] St. J. Hayes, St. A. Hinchliffe, J. D. Pope, P. Eccles, M. M. Khine, R. O. C. Kaschula, A. Sampedro, and D. van Velzen, Virchows Arch **427**, 101 (1995).
[34] A. R. Faruqui, H. N. Andrews, and C. Raeburn, Nucl. Instrum. Methods Phys. Res. A **348**, 659 (1994).
[35] J. Brink and W. Chiu, J. Struct. Biol. **113**, 23 (1994).
[36] Ch. Nicholson and L. Tao, Biophys. J. **65**, 2277 (1993).
[37] E. Maier, H. R. Crollius, and H. Lehrach, Nucl. Acids Res. **22**, 3423 (1994).
[38] Ch. Lengauer, R. M. Speicher, S. Popp, A. Jauch M. Taniwaki, R. Nagaraja, H. C. Riethman, H. Donis-Keller, M. D'Urso, D. Schlessinger, and Th. Cremer, Human Mol. Gen. **2**, 505 (1993).
[39] M. R. H. White, J. Morse, Z. A. M. Boniszewski, C. R. Mundy, M. A. W. Brady, and D. J. Chriswell, Technique **2**, 194 (1990).
[40] R. N. Waterhouse and L. N. Glover, Lett. Appl. Microbiol. **19**, 88 (1994).
[41] C. W. Earle, M. E. Baker, M. B. Denton, and R. S. Pomeroy, Trends Anal. Chem. **12**, 395 (1993).
[42] J. Castracane, L. P. Clow, S. Wegener, and G. Seidler, Rev. Sci. Instrum. **66**, 3668 (1995).
[43] Perkin Elmer, Nature (London) **381**, (1996).
[44] D. Lipson, N. G. Loebel, K. D. McLeaster, and B. Liu, IEEE Trans. Biomed. Eng. **BE-39**, 868 (1992).
[45] The rate constants κ are identical to the selection values (a measure for the fitness) in the quasispecies equation Ref. 13; if one sets the flux $\Phi(t) \approx 0$ and the portion of strands resulting from mutations $\Sigma_{j\neq k}\psi_{kj}c_j(t) \approx 0$, the following quasispecies equation is obtained (Refs. 13 and 47): $dc_k(t)/dt=(A_kQ_k-D_k)c_k(t)+\Sigma_{j\neq k}\psi_{kj}c_j(t)-\Phi(t);\quad k,j=1,\ldots,n$ becomes $c_k(t)/dt\approx(A_kQ_k-D_k)c_k(t)=\kappa c_k(t);\ k,j=1,\ldots n$.
[46] D. H. Ballard and C. M. Brown, *Computer Vision* (Prentice–Hall, Englewood Cliffs, NJ, 1982).
[47] TNO Institute of Applied Physics, TCL-IMAGE, users manual, 1991.
[48] G. Strunk, *Automatisierte Evolutionsexperimente und Natürliche Selektion unter Kontrollierten Bedingungen mit Hilfe der Serial-Transfer-Technik*, Thesis, Braunschweig (Verlag Shaker, Aachen, 1993).
[49] D. P. Bartel and J. W. Szostak, Science **261**, 411 (1993).
[50] A. A. Beaudry and G. F. Joyce, Science **257**, 63 (1992).
[51] Berzal-Herranz, A. S. Joseph, and J. M. Burke, Genes Dev. **6**, 129 (1992).
[52] A. D. Ellington and J. W. Szostak, Nature (London) **355**, 850 (1992).
[53] R. D. Jenison, S. C. Gill, A. Pardi, and B. Polisky, Science **263**, 1425 (1994).
[54] C. Tuerk and L. Gold, Science **249**, 505 (1990).
[55] A. Schober, *Strategien Einer Evolutiven Biotechnologie*, Thesis, Braunschweig (Verlag Shaker, Aachen, 1994).
[56] N. G. Walter and G. Strunk, Proc. Natl. Acad. Sci. USA **91**, 7937 (1994).
[57] A. Schober, M. Thürk, and M. Eigen, Biol. Cybern. **69**, 493 (1993).
[58] A. Schober, A. Schwienhorst, J. M. Koehler, M. Fuchs, R. Günther, and M. Thürk, Microsyst. Technol. **1**, 168 (1995).

This article is copyrighted as indicated in the article. Reuse of AIP content is subject to the terms at: http://scitationnew.aip.org/termsconditions. Downloaded to IP: 134.76.223.157 On: Tue, 06 Oct 2015 10:04:36